Conformational Heterogeneity of the Bacteriopheophytin Electron Acceptor H_A in Reaction Centers from *Rhodopseudomonas viridis* Revealed by Fourier Transform Infrared Spectroscopy and Site-Directed Mutagenesis

Jacques Breton,*,‡ Marina Bibikova,§,|| Dieter Oesterhelt,§ and Eliane Nabedryk‡

Section de Bioénergétique, Département de Biologie Cellulaire et Moléculaire, CEA/Saclay, 91191 Gif-sur-Yvette, France, and Max-Planck-Institut for Biochemistry, 82152 Martinsried, Germany

Received April 23, 1999; Revised Manuscript Received June 16, 1999

ABSTRACT: The light-induced Fourier transform infrared (FTIR) difference spectra corresponding to the photoreduction of either the H_A bacteriopheophytin electron acceptor (H_A^-/H_A spectrum) or the Q_A primary quinone (Q_A^-/Q_A spectrum) in photosynthetic reaction centers (RCs) of *Rhodopseudomonas viridis* are reported. These spectra have been compared for wild-type (WT) RCs and for two site-directed mutants in which the proposed interactions between the carbonyls on ring V of H_A and the RC protein have been altered. In the mutant EQ(L104), the putative hydrogen bond between the protein and the 9-keto C═O of H_A should be affected by changing Glu L104 to a Gln. In the mutant WF(M250), the van der Waals interactions between Trp M250 and the 10a-ester C═O of H_A should be modified. The characteristic effects of both mutations on the FTIR spectra support the proposed interactions and allow the IR modes of the 9-keto and 10a-ester C═O of H_A and H_A^- to be assigned. Comparison of the H_A^-/H_A and Q_A^-/Q_A spectra leads us to conclude that the Q_A^-/Q_A IR signals in the spectral range above 1700 cm^{-1} are largely dominated by contributions from the electrostatic response of the 10a-ester C═O mode of H_A upon Q_A photoreduction. A heterogeneity in the conformation of the 10a-ester C═O mode of H_A in WT RCs, leading to three distinct populations of H_A, appears to be related to differences in the hydrogen-bonding interactions between the carbonyls of ring V of H_A and the RC protein. The possibility that this structural heterogeneity is related to the observed multiexponential kinetics of electron transfer and the implications for primary processes are discussed. The effect of $^1H/^2H$ exchange on the Q_A^-/Q_A spectra of the WT and mutant RCs shows that neither Glu L104 nor any other exchangeable carboxylic residue changes appreciably its protonation state upon Q_A reduction.

In the reaction center (RC) of the photosynthetic purple bacterium *Rhodopseudomonas viridis*, the essential photochemical process involves the transfer of an electron from the primary donor P, a dimer of bacteriochlorophyll, via the monomeric bacteriochlorophyll molecule B_A, to the bacteriopheophytin (BPh) acceptor H_A in about 3 ps and then to the menaquinone Q_A in about 200 ps. The oxidized P is reduced in about 200 ns by a tightly bound tetraheme cytochrome subunit. When the redox potential is poised low enough so as to prereduce Q_A, continuous illumination of RCs allows the state H_A^- to be photoaccumulated.

The crystal structure of the RC of *Rps. viridis* (*1*−*4*) and of *Rhodobacter sphaeroides* (*5*−*10*) shows that the cofactors constituting P, B_A, H_A, and Q_A are anchored to a protein scaffold. For example, all the reported X-ray structures of bacterial RCs have concluded that the carboxylic acid side chain of the residue Glu L104 was within hydrogen-bonding distance of the 9-keto C═O group on ring V of H_A. Still another hydrogen bond between the 10a-ester C═O group, also on ring V of H_A, and the indole N−H of Trp L100 has been consistently proposed in all the structures (Figure 1). Similarly, hydrogen bonds of various strength anchoring the two carbonyls of Q_A have been reported from X-ray crystallography studies (*1*−*10*). In addition to this purely structural role, it is probable that the protein plays some specific function in assisting the electron transport and in preventing wasteful back reactions. Aromatic residues such as Tyr M208 located between P, B_A, and H_A or Trp M250 situated in van der Waals contact distance of both H_A and Q_A (*9*; Figure 1) have been pinpointed as playing a key role in the electron-transfer reactions (*11*−*15*). Structural rearrangements of the cofactors and of the RC protein are expected to contribute to the reorganization energy associated with long-range electron transfer. Indeed, the generation of the photosynthetic charges will affect the nuclear positions of the cofactors undergoing the oxidation/reduction steps themselves as well as of the polar groups that surround these cofactors. However, structural rearrangements could also occur at more distant sites, especially when considering that

* Corresponding author: Tel (331) 69 08 22 39; Fax (331) 69 08 87 17; e-mail cadara3@dsvidf.cea.fr.

‡ CEA/Saclay.

§ Max-Planck-Institut.

|| Present address: Department of Biochemistry, University of Utah Medical Center, Salt Lake City, UT 84132.

[1] Abbreviations: RC, reaction center; P, primary electron donor; B_A, monomeric bacteriochlorophyll on the active branch; H_A, bacteriopheophytin electron acceptor; Q_A (Q_B), primary (secondary) quinone acceptor; BPh, bacteriopheophytin; WT, wild type; FTIR, Fourier transform infrared; ENDOR, electron nuclear double resonance.

10.1021/bi990927f CCC: $18.00
Published on Web 08/12/1999

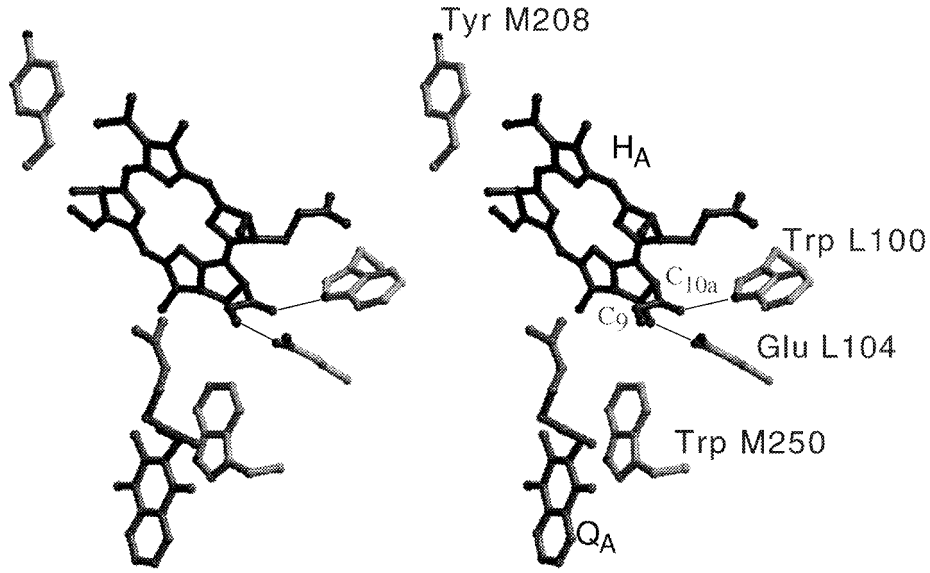

FIGURE 1: Stereoview of the environment of ring V of the bacteriopheophytin electron acceptor H_A in the photosynthetic reaction center of *Rps. viridis*, depicting hydrogen bonds between the 9-keto and 10a-ester C═O of H_A and the residues Glu L104 and Trp L100, respectively. Also shown are the primary quinone Q_A and the residues Trp M250 and Tyr M208. The structure is oriented with the C_2 axis approximately vertical. The phytyl and isoprenoid chains of H_A and Q_A have been truncated for clarity. The coordinates shown are from Brookhaven National Laboratory file 1PRC.

the movement of charged groups in response to the change of local electrostatic field could propagate over rather long distances. Specific information on such local and/or distant response of the protein medium and of the other cofactors upon electron transfer is still quite scarce.

It has been previously shown that light-induced FTIR difference spectroscopy has the potential to reveal changes of the individual atomic bonds that are altered by the charge separation process. Notably, the IR spectral changes associated with the photoreduction of either H_A (*16*−*19*) or Q_A (*20*−*22*) in *Rps. viridis* have been well characterized. Comparison of these light-induced difference spectra with the redox-induced difference spectra of the relevant model compounds for the cofactors in solution provides a guideline for interpreting the spectra (*17*, *19*, *23*). A firmer assignment of the bands can be obtained whenever either a given type of amino acid residue or the native cofactor itself can be replaced by an isotopomer (*22*, *24*). However, a more general and technically amenable way to analyze the role of some side chains or to gauge possible interactions between amino acid residues and the cofactors is to use site-directed mutagenesis. In this approach, the X-ray model of the RC is used to target specific groups of the protein that appear to interact with a given cofactor. This approach has been developed to probe the bonding interactions of P with the protein (reviewed in ref *25*). When combined with $^1H/^2H$ exchange experiments, it has been also applied to the investigation of several of the carboxylic residues that could be involved in proton uptake upon photoreduction of the secondary quinone Q_B in *Rb. sphaeroides* (*26*, *27*). In this case, interpretation of the results relies on the fact that (i) the C═O mode of protonated carboxylic acid side chains absorbs between 1770 and 1700 cm^{-1} in a frequency region where the C═O mode of ester compounds are the only other potential contributors and (ii) the C═O mode of carboxylic groups involved in proton-transfer reaction should be sensitive to $^1H/^2H$ exchange and therefore it is expected to downshift by about 4−12 cm^{-1} after the RCs have been incubated in ^2H_2O (*26*−*29*). Such FTIR measurements appear at present well-suited to help evaluate the results of the electrostatic calculations that have been performed on both RCs for which a X-ray model is available, namely, those of *Rb. sphaeroides* (*30*−*32*) and *Rps. viridis* (*33*, *34*).

Recently, the photoreduction of Q_A in *Rb. sphaeroides* RCs bearing mutations at Glu L104 and/or Trp L100 has been investigated by FTIR difference spectroscopy, leading to the conclusion that the protons taken up in substoichiometric amounts upon Q_A reduction were not localized on carboxylic acid residues (*35*). Furthermore, an electrostatic influence of Q_A photoreduction on the vibrational mode of the 10a-ester C═O group on ring V of H_A was described. In this study it was further concluded that this carbonyl group occupies a number of different conformations (*35*). Such heterogeneity of the H_A conformation should show up clearly in the FTIR spectra corresponding to the photoreduction of H_A, insofar as the 10a-ester C═O group of this cofactor is known to contribute to the difference spectra (*18*). However, in the FTIR study of the *Rb. sphaeroides* RC mutants (*35*) it had not been possible to perform the photoreduction of H_A, thus impeding a correlation between the contribution of the 10a-ester C═O in the H_A^-/H_A and Q_A^-/Q_A spectra. The existence of a tightly bound cytochrome in *Rps. viridis* considerably facilitates the photoreduction of H_A.

In the present study, the FTIR difference spectra of Q_A photoreduction and of H_A photoreduction in isolated RCs of *Rps. viridis* are compared for WT and for site-directed mutants involving two key residues interacting with H_A and/or Q_A, namely, Glu L104 and Trp M250. Assignments are proposed for the IR bands corresponding to the 9-keto and 10a-ester C═O vibrations of both H_A and H_A^- in WT and in the mutants. The electrostatic influence of the Q_A^- charge on the 10a-ester C═O vibration of H_A is analyzed. The results are interpreted in terms of a substantial heterogeneity of the conformation of ring V of H_A in the RC of *Rps. viridis*. The effect of $^1H/^2H$ exchange shows that the state of protonation of carboxylic acid residues does not change

appreciably upon Q_A reduction. A preliminary account of some of these results has been presented (*36*).

MATERIALS AND METHODS

The mutant strains EQ(L104) and WF(M250) or WY(M250) contain the change Glu to Gln at residue L104 and Trp to Phe or Tyr at residue M250, respectively. Mutants were prepared by the Kunkel method of site-specific mutagenesis using uracil-containing DNA (*37*). Mutated fragments were cloned into the broad host range vector pRK404, which is stably maintained in *Rps. viridis*. The *Escherichia coli* strain S17-1 was used to mobilize pRK404 into *Rps. viridis* by a conjugation procedure (*38*). *Rps. viridis* mutants were grown photoheterotrophically in N-medium. The introduced mutations were confirmed for all the mutants by sequence analysis of the DNA isolated from the cell batch used for the isolation of the RCs.

The RC samples were isolated in 15 mM Tris-HCl, pH 8, and 0.025% lauryldimethylamine *N*-oxide as previously described (*39*). For $^1H/^2H$ exchange, the RCs were resuspended three times into ^2H_2O at 20 °C and the solvent was evaporated under argon. This procedure leads to about 70% ^2H-labeling of the NH peptide groups. Control experiments were performed under the same conditions with the RCs suspended in ^1H_2O. Light-induced FTIR measurements (Nicolet 60SX) were performed under saturating steady-state illumination, with an alternating sequence of 23 s dark, 23 s light, and 23 s dark. For a given sample these cycles were continuously repeated over 6−12 h. A batch representing the different sample conditions (wt, mutant, ^1H_2O, ^2H_2O) was prepared and the samples were alternatively measured for a total of 3−5 days. The spectra presented correspond to an average of the data taken on 2−3 different batches. For H_A reduction, the RC sample set at −20 °C in Tris buffer (100 mM; pH 8) contained 100 mM dithiothreitol and 20 mM *N*,*N*,*N*′,*N*′-tetramethyl-1,4-phenylenediamine (*18*). For Q_A reduction, the RC sample set at 5 °C in Tris buffer (100 mM; pH 7) contained 20 mM of the mediator 2,3,5,6-tetramethyl-1,4-phenylenediamine and 10 mM ascorbate as reported previously (*20*, *22*), except that stigmatellin (2 mM) was used instead of *o*-phenanthroline to inhibit electron transfer to Q_B. For the ^2H_2O samples, the Tris/mediator/ascorbate/stigmatellin mixture was prepared in ^2H_2O.

RESULTS

The H_A^-/H_A light minus dark FTIR difference spectra of RCs isolated from *Rps. viridis* WT and from the EQ(L104) and WF(M250) mutants are shown in Figure 2, spectra a−c, respectively. In these spectra the negative bands pertain to the vibrations from the H_A state and the positive bands belong to those of the H_A^- state. The spectrum of WT RCs is very close to those previously reported (*16*−*19*). The spectra of the mutants differ from that of WT, notably between 1750 and 1560 cm^{-1}. These differences are best visualized by calculating a double-difference spectrum (WT minus mutant) between two individual H_A^-/H_A spectra upon minimization of the residual signals in the whole spectral range of the measurement (1800−1000 cm^{-1}). Such spectra are depicted in Figure 3 in the 1760−1540 cm^{-1} frequency range. In these double-difference spectra, interactive subtraction of the two parent spectra is used to obtain the smallest possible peak-to-peak amplitude for all the bands. It is observed that this normalization also leads to the strong reduction or the almost complete disappearance of a number of bands such as those at 1747 cm^{-1} (Figure 3a) or at 1602−1595 cm^{-1} (Figure 3b) as well as those at 1659, 1530, 1470, and 1369 cm^{-1} (Figure 2) and at 1158 cm^{-1} (not shown). The shape of the double-difference spectra was consistently reproduced when different sets of H_A^-/H_A spectra obtained for RC samples corresponding to identical experimental conditions were used. Finally, variations by ±10% of the optimum coefficient selected from the interactive subtraction do not lead to a significant perturbation of the double-difference spectra (data not shown), in particular for those bands that bear a frequency label (Figure 3), which are discussed in the following.

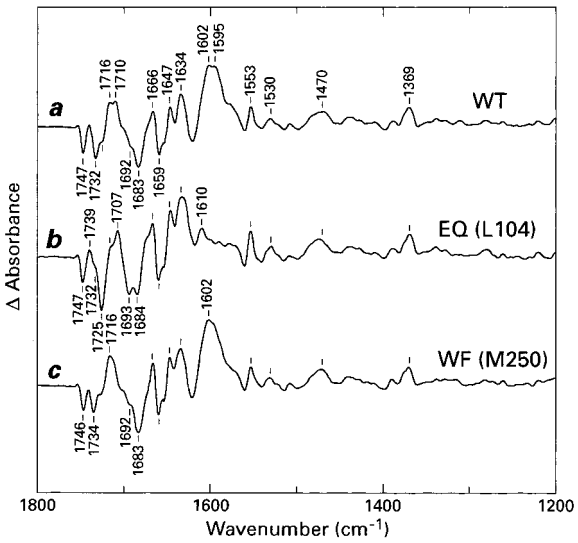

FIGURE 2: Light-induced H_A^-/H_A FTIR difference spectra of *Rps. viridis* RCs (a) WT, (b) EQ(L104) mutant, and (c) WF(M250) mutant. Spectral resolution was 4 cm^{-1}; about 100 000 interferograms were added. The frequency of the IR bands is given at ±1 cm^{-1}. In spectrum a the peak-to-peak amplitude is 8×10^{-4} absorbance unit.

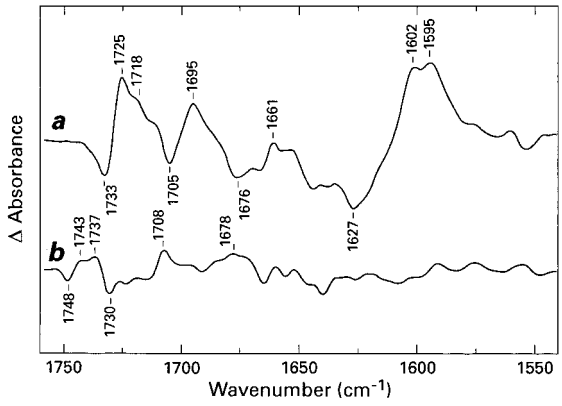

FIGURE 3: WT minus mutant double-difference spectra calculated from H_A^-/H_A spectra shown in Figure 2. (a) WT minus EQ(L104); (b) WT minus WF(M250).

The mutation EQ(L104), in which Glu L104 has been replaced by a glutamine residue, should eliminate the possible contribution to the IR spectra of the carboxylic acid side chain and should suppress, or at least alter, any indirect effect brought about by the hydrogen bond to the 9-keto C═O of H_A. The most noticeable differences between the H_A^-/H_A spectra of WT and the EQ(L104) mutant (Figure 2a,b) are

the disappearance in the mutant of the large positive band at ≈1600 cm^{-1} of WT and the increase in the mutant of the negative bands at 1693 and 1725 cm^{-1}. While the parent spectra for WT and the EQ(L104) mutant are quite complicated in the frequency region above 1540 cm^{-1} (Figure 2a,b), the comparison of these spectra with the double-difference spectrum (Figure 3a), taking especially into account the positive or negative sign of the bands, shows that most of the differential-shaped features in the double-difference spectra can be explain by frequency shifts of a rather simple set of bands. Notably, the 1733(−)/1725(+) cm^{-1} differential signal (Figure 3a) originates from a downshift of the negative band at 1732 cm^{-1} in Figure 2a to 1725 cm^{-1} upon the EQ(L104) mutation. The shoulder at 1718 cm^{-1} and the negative band at 1705 cm^{-1} (Figure 3a) can probably be related to the downshift of a positive band at 1716 cm^{-1} in WT. The 1695(+)/1676(−) cm^{-1} differential signal seems to originate from the large increase of a negative band at 1693 cm^{-1} in the spectrum of the mutant. It should thus correspond to the upshift upon mutation of a negative band around 1676 cm^{-1} in WT, although this band is not clearly visible in the H_A^-/H_A spectrum (Figure 2a). Finally, the large 1627(−)/1602−1595(+) cm^{-1} differential signal can be assigned to the upshift of the positive band around 1600 cm^{-1} in the WT spectra upon the EQ(L104) mutation.

A somewhat surprising observation related to the set of bands in the H_A^-/H_A spectra of WT and EQ(L104) mutant RCs discussed above is the presence in the H_A^-/H_A spectra of the WT RCs (Figure 2a) of small bands at the same frequencies as in the mutant spectra (Figure 2b). Similarly, several bands that are well developed in the WT spectra are present with a small amplitude in the mutant spectra. For example, the main 1732 cm^{-1} band of WT has a small replica in the mutant spectra, while a shoulder under the main 1725 cm^{-1} band of the mutant is seen in the WT spectra. In addition, a set of two positive bands with different relative amplitudes is found in the 1720−1700 cm^{-1} range in both the WT and the mutant spectra. In an analogous way, negative bands at about 1693 and 1683 cm^{-1} as well as a positive band at 1634 cm^{-1} are found in both spectra. While the complex character of the FTIR difference spectra with many overlapping positive and negative bands could lead to the fortuitous appearance of unrelated bands at the same frequency in the WT and mutant spectra, their mere repetition is surprising. Assuming that these bands are indeed related, one would be led to invoke some heterogeneity in the vibrations, and thus the bonding pattern, of H_A in WT and in the EQ(L104) mutant.

The impact of the WF(M250) mutation on the H_A^-/H_A spectrum (Figures 2c and 3b) is less pronounced than that of the EQ(L104) mutation, indicating a smaller perturbation than that induced by the rupture of the hydrogen bond to the 9-keto C═O of H_A. This result is consistent with the van der Waals nature of the interaction between Trp M250 and H_A described in the X-ray model of the RC. The main effects observed upon mutation are the ≈2 cm^{-1} upshift of the band at 1732 cm^{-1} and a small amplitude decrease of a band at 1710 cm^{-1}. In addition there is a very small downshift (≈1 cm^{-1}) of the band at 1747 cm^{-1}. The large positive band at ≈1600 cm^{-1} remains unaffected by the mutation. Very comparable results have been obtained with the WY(M250) mutant (data not shown).

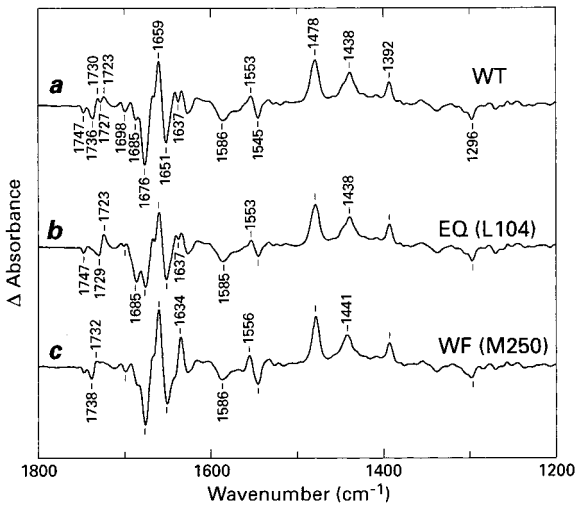

FIGURE 4: Light-induced Q_A^-/Q_A FTIR difference spectra in ^1H_2O of *Rps. viridis* RCs (a) WT, (b) EQ(L104) mutant, and (c) WF(M250) mutant. In spectrum a the peak-to-peak amplitude is 2.4×10^{-3} absorbance unit.

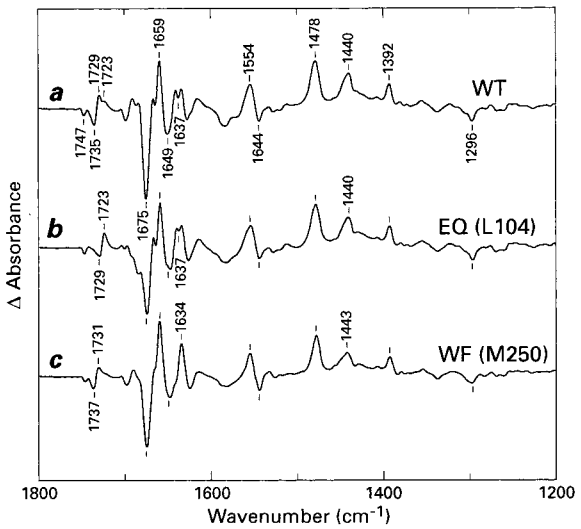

FIGURE 5: Light-induced Q_A^-/Q_A FTIR difference spectra in ^2H_2O of *Rps. viridis* RCs (a) WT, (b) EQ(L104) mutant, and (c) WF(M250) mutant. In spectrum a the peak-to-peak amplitude is 3.3×10^{-3} absorbance unit.

The Q_A^-/Q_A light minus dark FTIR difference spectra in ^1H_2O of RCs isolated from *Rps. viridis* WT and from the EQ(L104) and WF(M250) mutants are shown in Figure 4, spectra a−c, respectively. The corresponding spectra after the RCs have been incubated in ^2H_2O are depicted in Figure 5, spectra a−c, respectively. The spectra of WT RCs are very close to those previously reported (*20*, *22*, *40*, *41*). The spectra of the mutants differ from those of WT, notably between 1750 and 1630 cm^{-1} as best visualized in the WT minus mutant double-difference spectra (Figure 6). The ^1H_2O minus ^2H_2O double-difference spectra are shown in Figure 7. The most noticeable differences between the Q_A^-/Q_A spectra of WT and of the EQ(L104) mutant (Figures 4a,b and 5a,b) are the amplitude decrease of the negative band at 1676 cm^{-1} with the increase of the negative band at 1685 cm^{-1} upon mutation as well as the prominent changes in the 1740−1720 cm^{-1} frequency range. The double-difference spectra (Figure 6a,b) reveal primarily a complex signal representing the overlap of two bandshifts responsible for

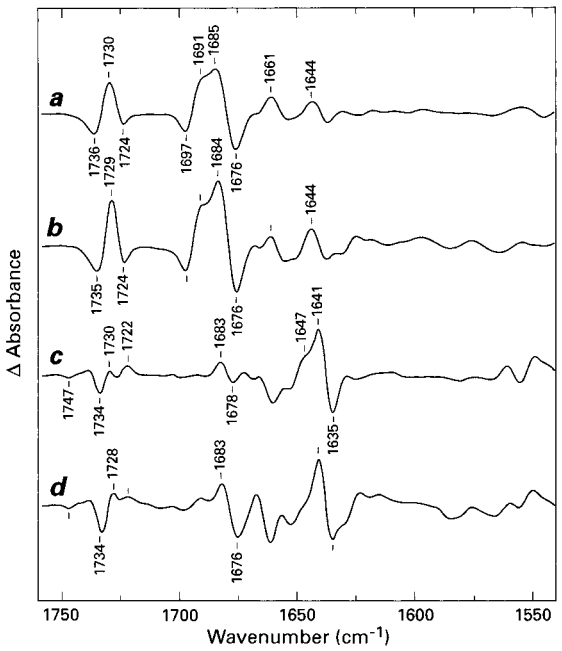

FIGURE 6: WT minus mutant double-difference spectra calculated from Q_A^-/Q_A spectra shown in Figures 4 and 5. (a) WT minus EQ(L104) in ^1H_2O; (b) WT minus EQ(L104) in ^2H_2O; (c) WT minus WF(M250) in ^1H_2O; (d) WT minus WF(M250) in ^2H_2O.

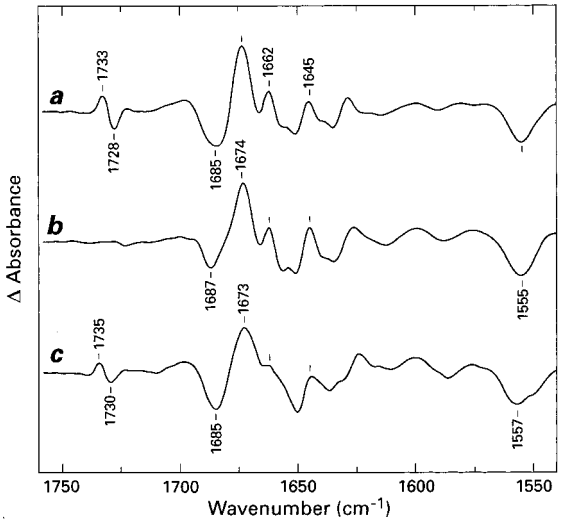

FIGURE 7: ^1H_2O minus ^2H_2O double-difference spectra calculated from Q_A^-/Q_A spectra shown in Figures 4 and 5. (a) WT; (b) EQ(L104) mutant; (c) WF(M250) mutant.

the negative bands at 1697 and 1676 cm^{-1} and the positive peak at ≈1685 cm^{-1} with a shoulder at 1691 cm^{-1} and another signal with a second-derivative shape centered at ≈1730 cm^{-1}. The second-derivative shape of this signal (Figure 6a,b) suggests that it could originate from the sharpening upon Q_A reduction of a band centered close to 1730 cm^{-1} in WT, which would be absent in the mutant. However, when the double-difference spectra are compared to the parent spectra this feature appears more likely to result from the overlap of two derivative signals of opposite signs and centered at ≈1733 and 1726 cm^{-1}, reflecting the shift upon mutation of a differential signal present at 1736(−)/1730(+) cm^{-1} in WT (Figure 4a) and at 1729(−)/1723(+) cm^{-1} in the mutant (Figure 4b).

The same observation relative to the unexpected presence of bands at the same frequency in the spectra of the WT and of the EQ(L104) mutant that was made earlier for the H_A^-/H_A spectra repeats itself when the Q_A^-/Q_A spectra of WT and of the mutant are compared (Figures 4a,b and 5a,b). Notably, bands at 1676, 1685, 1698, and 1723 cm^{-1}, which change amplitude upon mutation, are common to both spectra. These observations will be discussed in a later section.

Comparison of the WT minus WF(M250) Q_A^-/Q_A double-difference spectrum (Figure 6c) and of the parent spectra in ^1H_2O (Figure 4a,c) shows that above 1650 cm^{-1} the main perturbations with respect to WT RCs are a ≈2 cm^{-1} upshift of the differential signal centered at 1733 cm^{-1}, a decrease of a small 1727(−)/1723(+) cm^{-1} differential feature, and the appearance of a differential signal negative at 1678 and positive at 1683 cm^{-1} (Figure 6c). Very comparable spectra have been obtained with the WY(M250) mutant (data not shown). On the basis of experiments in which the primary quinone Q_A has been exchanged with vitamin K_1 bearing various isotopic labels in both WT *Rps. viridis* RCs (*24*) and in the WF(M250) mutant (unpublished results), the positive band peaking at 1641 cm^{-1} with a shoulder at 1647 cm^{-1} and an associated negative band at 1635 cm^{-1} (Figure 6c) is assigned to small shifts of Q_A carbonyl vibrational modes.

The Q_A^-/Q_A spectra for RCs that have been incubated in ^2H_2O (Figure 5) are slightly different from those of RCs that have been incubated in ^1H_2O (Figure 4) for both WT and the EQ(L104) and WF(M250) mutants. Further information on the effect of $^1H/^2H$ exchange can be obtained from these spectra by comparison of the WT minus mutant double-difference spectra (Figure 6) or of the corresponding ^1H_2O minus ^2H_2O double-difference spectra (Figure 7). The WT minus EQ(L104) double-difference spectrum calculated for the RCs incubated in ^2H_2O (Figure 6b) is close in shape to that measured in ^1H_2O (Figure 6a). The main difference is the amplitude increase in ^2H_2O of the complex differential signals at 1736(−)/1730(+)/1724(−) and 1697(−)/1685(+)/1676(−) cm^{-1}. In the region around 1730 cm^{-1}, $^1H/^2H$ exchange also induces a 1 cm^{-1} downshift of the 1736/1730 cm^{-1} differential signal. The ^1H_2O minus ^2H_2O double-difference spectra for WT and for the mutants (Figure 7) are close in the 1700−1500 cm^{-1} frequency region. They display a negative band at ≈1555 cm^{-1} in the region of the amide II absorption and a ≈1685(−)/1674(+) cm^{-1} differential signal. However, they differ significantly in the region above 1700 cm^{-1}. Notably, a mostly differential signal, positive at 1733 cm^{-1} and negative at 1728 cm^{-1}, observed in the ^1H_2O minus ^2H_2O double-difference spectrum for WT (Figure 7a) is upshifted by ≈2 cm^{-1} in the WF(M250) mutant (Figure 7c) but is essentially absent in the corresponding spectrum for the EQ(L104) mutant (Figure 7b). The disappearance upon EQ(L104) mutation of the 1733/1728 cm^{-1} differential signal induced by $^1H/^2H$ exchange in WT inescapably points to an involvement of Glu L104 in these IR spectral changes. However, this observation does not clearly indicate whether these changes upon Q_A reduction should be related simply to an electrostatic perturbation of the C═O mode of the protonated Glu L104 side chain in WT RCs or if they are rather due to some indirect effect of $^1H/^2H$ exchange or of the mutation at Glu L104 on a nearby vibration. The finding that the differential signal at 1733/1728 cm^{-1} is upshifted by ≈2 cm^{-1} and affected in its

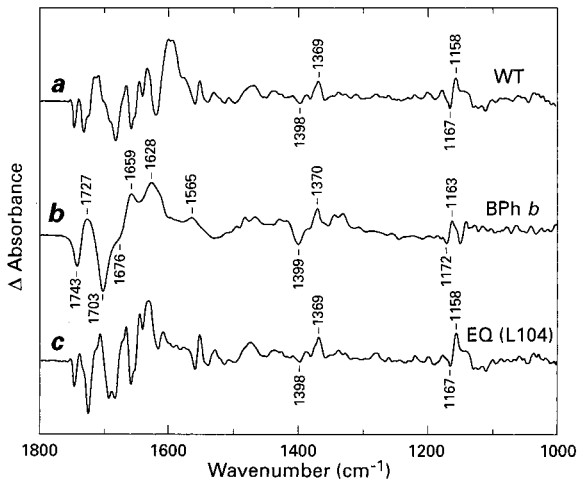

FIGURE 8: (a) Light-induced H_A^-/H_A FTIR difference spectrum of WT *Rps. viridis* RCs. (b) Electrochemically induced BPh b^-/BPh *b* FTIR difference spectrum of bacteriopheophytin *b* in deuterated tetrahydrofuran. (c) Light-induced H_A^-/H_A FTIR difference spectrum of *Rps. viridis* EQ(L104) RCs mutant. The peak-to-peak amplitudes are 8×10^{-4} and 0.23 absorbance units in spectra a and b, respectively.

amplitude in the ^1H_2O minus ^2H_2O double-difference spectrum for the WF(M250) mutant (Figure 7c) does not favor the former interpretation inasmuch as the change of a Trp by a Phe side chain at M250 should not affect the vibrational frequency of the C═O mode of the protonated Glu L104 side chain.

DISCUSSION

Although the H_A^-/H_A spectra of RCs of WT *Rps. viridis* (Figures 2a and 8a) and of the EQ(L104) mutant (Figures 2b and 8c) are quite different, they both show a strong overall analogy with the BPh b^-/BPh *b* difference spectrum (Figure 8b), corresponding to the electrochemical reduction of BPh *b* in deuterated tetrahydrofuran (*19*). On one hand, the large effect that the mutation induces on the H_A^-/H_A spectra could be expected, taking into account the rupture of a hydrogen bond to the 9-keto C═O group of H_A targeted by the mutation together with the high extinction coefficient of keto groups in the IR and the known sensitivity of these modes to hydrogen-bonding effects (*42*, *43*). Thus, in the following section, the effect of the EQ(L104) mutation on the spectra will be analyzed to propose an assignment of the C═O modes of H_A and H_A^- in WT and mutant RCs. On the other hand, the relatively large perturbations that the EQ(L104) mutation induces in the region 1750−1670 cm^{-1} of the Q_A^-/Q_A spectra were not expected as the mutation site is quite far (about 10 Å away) from the primary quinone. It is worth noting, however, that the largest changes induced by the mutation in the Q_A^-/Q_A WT minus EQ(L104) double-difference spectra (Figure 6a), i.e., the second-derivative signal centered at 1730 cm^{-1} and the complex feature extending between 1700 and 1670 cm^{-1}, are found at frequencies where large differential features are seen in the corresponding H_A^-/H_A double-difference spectrum (Figure 3a). Similarly, changes are observed around 1730 and 1678 cm^{-1} in both the H_A^-/H_A and Q_A^-/Q_A WT minus WF(M250) double-difference spectra although they are of a smaller amplitude than those elicited by the EQ(L104) mutation. In the following, it will be shown that the differential signals of the WT minus mutant H_A^-/H_A spectra (Figure 3) can be primarily assigned to frequency shifts of the 10a-ester and 9-keto C═O bands of H_A and H_A^- in response to the mutations. The corresponding signals observed in the Q_A^-/Q_A WT minus mutant double-difference spectra (Figure 6) can be rationalized by taking into account the additional electrostatic influence of Q_A photoreduction on the C═O groups attached to ring V of H_A previously considered to analyze the Q_A^-/Q_A spectra of *Rb. sphaeroides* RCs bearing mutations at the Glu L104 and/or Trp L100 sites (*35*).

Assignment of the BPh Bands in the H_A^-/H_A Spectra. In a previous study, the H_A^-/H_A spectra of *Rb. sphaeroides* and *Rps. viridis* RCs were shown to be highly similar (*18*). Comparing these spectra with the BPh^-/BPh difference spectra of the isolated pigments, it was deduced that the 9-keto carbonyl was hydrogen-bonded in both the H_A and H_A^- states, absorbing at ≈1680 and 1590−1600 cm^{-1}, respectively. The two bands, negative at 1732 cm^{-1} and positive at ≈1710 cm^{-1}, were assigned to a bound ester C═O group of H_A and H_A^-, respectively. The negative band at 1747 cm^{-1} was tentatively attributed to a free ester C═O together with a weak contribution of the COOH group of Glu L104 in the 1745−1735 cm^{-1} frequency range. These assignments were in line with previous interpretations (*16*, *17*, *19*).

Concerning the 9-keto C═O group of H_A, the effect of the EQ(L104) mutation on the H_A^-/H_A spectra of *Rps. viridis* RCs is consistent with the previous assignments discussed above and further confirms the presence of a hydrogen bond between the COOH of Glu L104 and the 9-keto C═O of H_A proposed from the X-ray data (*1*−*4*). The FTIR data are also in agreement with the presence of a hydrogen bond in the H_A^- state of WT RCs previously deduced from ENDOR measurements (*44*). Notably, the large increase of the negative band at 1693 cm^{-1} and the disappearance of the positive band at ≈1600 cm^{-1} in the EQ(L104) mutant spectra (Figure 2b) provide evidence for a rupture or, at least, a strong perturbation of the hydrogen bond to the 9-keto C═O of both H_A and H_A^- in the mutant. In addition, the WT minus mutant double-difference spectrum (Figure 3a) shows that upon EQ(L104) mutation the 9-keto C═O group of H_A shifts from 1676 to 1695 cm^{-1} for the neutral state and from ≈1600 to 1627 cm^{-1} for the anion state. On the other hand, no significant effect of the WF(M250) mutation on the 9-keto C═O group of H_A is detected (Figure 3b), showing that Glu L104 is also hydrogen-bonded in WF(M250). The 1676 cm^{-1} frequency found for the 9-keto C═O group of WT is in good agreement with that (1678 cm^{-1}) reported in a resonance Raman study of *Rps. viridis* RCs (*45*). The frequency observed for the 9-keto C═O of H_A in the EQ(L104) mutant is slightly lower (by ≈10 cm^{-1}) than that of BPh *b* in tetrahydrofuran, suggesting a more polar environment in the RC than in solution. This is consistent with the presence of the Gln side chain in the mutant. It is not possible from the present data to rule out the presence of a weak hydrogen bond to the amine group of the Gln side chain. However, it should be stressed that the electron density on ring V of H_A, and therefore the frequency of the 9-keto C═O, depends on many other environmental factors that affect the conformation of the whole molecule (*35*, *46*).

In principle the negative bands at 1747 and 1732 cm^{-1} in the H_A^-/H_A spectra of WT *Rps. viridis* RCs could represent

contributions from the 10a-ester C═O group of H_A and the COOH group of Glu L104, which are both expected to absorb in the 1760−1700 cm^{-1} frequency range. A much less likely contribution from the 7c-ester C═O cannot be strictly ruled out but will not be further discussed as the anion minus neutral IR difference spectra of Phe *a* and of its pyro derivative show that this ester group is insensitive to the reduction of the macrocycle (*47*). Upon the EQ(L104) mutation, the 1747 cm^{-1} band is unaffected while the 1732 cm^{-1} band appears to downshift to 1725 cm^{-1}. For the COOH mode of Glu L104 to contribute directly to the FTIR difference spectra, the corresponding band would have to shift from 1732 to 1725 cm^{-1} upon H_A photoreduction in WT RCs. However, two observations make this proposal rather unlikely. First, the extremely small magnitude of the effect of $^1H/^2H$ exchange on the 1732 cm^{-1} signal, that shifts by at most 1 cm^{-1} upon exchange (data not shown), is inconsistent with an assignment of this signal to a protonated Glu L104 carboxylic group that has been shown to exchange (*44*). Second, the finding that the WF(M250) mutation, which involves a residue with no direct interaction with Glu L104 (Figure 1), also affects the 1732 cm^{-1} band is difficult to reconcile with the possibility that this band corresponds to vibrations from Glu L104. On the other hand, these two observations leave open the possibility that the EQ(L104) mutation affects the 10a-ester C═O group of H_A, downshifting its frequency from 1732 to 1725 cm^{-1}. In a previous study of the Q_A^-/Q_A spectra of WT *Rb. sphaeroides* and of mutants at the Glu L104 and Trp L100 sites, it was concluded that the 10a-ester C═O group of H_A can afford several distinct conformations. It was further observed that the equilibrium between these different populations is under the influence of two hydrogen-bonding interactions between, on one hand, Glu L104 and the 9-keto C═O and, on the other hand, Trp L100 and the 10a-ester C═O (*35*). The close correspondence between the H_A^-/H_A spectra of *Rb. sphaeroides* and *Rps. viridis* RCs (*18*) makes it highly likely that the details of the conformation of H_A are very close in the RCs of the two species. Thus, it can be proposed that the 1747 and 1732 cm^{-1} bands in the H_A^-/H_A spectra of WT *Rps. viridis* RCs also represent two main populations of the 10a-ester C═O group of H_A that differ by their conformation. The finding that the WF(M250) mutation affects vibrations from the 10a-ester C═O group of H_A in the 1750−1730 cm^{-1} region is consistent with this proposal insofar as this residue is located within van der Waals interaction of the ring V of H_A on the side of the 10a-carbomethoxy group and is pointing toward that group (Figure 1). The H_A band at 1747 cm^{-1}, insensitive to the EQ(L104) mutation, is close in frequency to the band at 1743 cm^{-1} of the 10a-ester C═O group of BPh *b* in tetrahydrofuran (Figure 8b). Positive contributions from the different populations of the 10a-ester C═O group in the H_A^- state can be seen at 1739, 1716, and 1710−1707 cm^{-1} (Figure 2). The possibility that the shoulder observed at ≈1725 cm^{-1} in the H_A^-/H_A spectra of WT *Rps. viridis* RCs corresponds to a third population of the 10a-ester C═O group of H_A as well as a rationale for the proposal of heterogeneous conformation of this group will be further discussed in a following section.

Electrostatic Influence of Q_A Reduction on the Vibrations of H_A. In the region above 1700 cm^{-1}, a negative band at 1747 cm^{-1} is present in both the H_A^-/H_A and the Q_A^-/Q_A spectra of WT *Rps. viridis* RCs (Figures 2a and 4a). The position and the amplitude of this band are unaffected by the EQ(L104) mutation (Figures 2b and 4b). A band at almost the same frequency is also present in the H_A^-/H_A spectrum of WT *Rb. sphaeroides* RCs (*18*) and in the Q_A^-/Q_A spectra of WT *Rb. sphaeroides* RCs as well as of *Rb. sphaeroides* RCs bearing the EL(L104) mutation (*35*). When the mutation WF(L100) that prevents the formation of the hydrogen bond to the 10a-ester C═O group of H_A is introduced in *Rb. sphaeroides*, the 1747 cm^{-1} band in the Q_A^-/Q_A spectra becomes severely affected. It gives rise to a strong differential signal negative at 1745 cm^{-1} and positive at 1739 cm^{-1}, while the amplitude of a differential signal centered at ≈1731 cm^{-1} in WT decreases (*35*). The large influence of the WF(L100) mutation on the 1747 cm^{-1} band of the Q_A^-/Q_A spectra in *Rb. sphaeroides* has been the main observation leading to the proposal of an electrostatic response of the vibration of the 10a-ester C═O group of H_A upon reduction of Q_A (*35*). The presence of the 1747 cm^{-1} band in the Q_A^-/Q_A spectra of WT *Rb. sphaeroides* and *Rps. viridis* as well as the comparable lack of sensitivity of this band to $^1H/^2H$ exchange or to mutations that remove the Glu L104 side chain in both species lead us to make the same proposal for the origin of this band also in *Rps. viridis*.

A differential signal, negative at 1736 cm^{-1} and positive at 1730 cm^{-1}, in the Q_A^-/Q_A spectra of WT *Rps. viridis* RCs is centered close to the negative band peaking at 1732 cm^{-1} in the H_A^-/H_A spectra. Most notably, the 7 cm^{-1} downshift of the differential signal in the Q_A^-/Q_A spectra occurring upon the EQ(L104) mutation (Figure 4a,b) parallels the downshift of the corresponding H_A band from 1732 to 1725 cm^{-1} (Figure 2a,b). Similarly, the 2 cm^{-1} upshift of this differential signal occurring upon the WF(M250) mutation (Figure 4c) parallels the upshift of the corresponding H_A band from 1732 to 1734 cm^{-1} (Figure 2c). In the Q_A^-/Q_A spectrum of *Rb. sphaeroides*, a downshift by ≈7 cm^{-1} of a differential feature at 1735(−)/1728(+) cm^{-1} has been documented upon EL(L104) mutation. This differential feature in WT *Rb. sphaeroides* has been assigned to the electrostatic response of the vibration of a second population of the 10a-ester C═O group of H_A upon reduction of Q_A (*35*). The parallel behavior upon either the EQ(L104) or the WF(M250) mutation of the spectral features centered around 1732 cm^{-1} in both the Q_A^-/Q_A and the H_A^-/H_A spectra of WT *Rps. viridis* RCs strongly supports the same assignment to be made also in this species for the corresponding 1736(−)/1730(+) cm^{-1} signal.

The ^1H_2O minus ^2H_2O Q_A^-/Q_A double-difference spectrum exhibits a differential signal at 1730(+)/1724(−) cm^{-1} for WT *Rb. sphaeroides* (*35*, *40*) and at 1733(+)/1728(−) cm^{-1} for WT *Rps. viridis* (*40*; Figure 7a). This signal disappears in the case of the EQ(L104) mutant of *Rps. viridis* (Figure 7b) and upshifts by about 2 cm^{-1} in the WF(M250) mutant (Figure 7c). Similarly, the 1730(+)/1724(−) cm^{-1} signal in WT *Rb. sphaeroides* disappears in the EL(L104) mutant (*35*). At first sight one could be tempted to interpret these $^1H/^2H$ exchange-induced differential signals that disappear upon mutating Glu L104 as due to the downshift upon $^1H/^2H$ exchange of the C═O mode of the Glu L104 side chain. However, inspection of the Q_A^-/Q_A spectra of WT *Rps. viridis* in ^1H_2O and in ^2H_2O (Figures 4a and 5a) reveals that the 1733(+)/1728(−) cm^{-1} differential signal depicted in

Figure 7a indeed originates from the ≈1 cm^{-1} downshift upon $^1H/^2H$ exchange of the differential signal at 1736(−)/1730(+) cm^{-1}. Similarly, the 1735(−)/1728(+) cm^{-1} differential signal in the Q_A^-/Q_A spectra of WT *Rb. sphaeroides* is downshifted by ≈1 cm^{-1} upon $^1H/^2H$ exchange (*35*, *40*). When the RCs bear a mutation at the Glu L104 site, the corresponding signals at 1727(−)/1722(+) cm^{-1} in EL(L104) *Rb. sphaeroides* (*35*) and at 1729(−)/1723(+) cm^{-1} in EQ(L104) *Rps. viridis* (Figures 4b and 5b) are unaffected by $^1H/^2H$ exchange. On the other hand, the same downshift by ≈1 cm^{-1} upon $^1H/^2H$ exchange is also observed for the 1738(−)/1732(+) cm^{-1} differential signal of the WF(M250) mutant of *Rps. viridis* (Figures 4c and 5c).

As noted previously for the Q_A^-/Q_A spectra of *Rb. sphaeroides* (*35*), the ≈1 cm^{-1} shift upon $^1H/^2H$ exchange of the 1736(−)/1730(+) cm^{-1} differential signal in the Q_A^-/Q_A spectra of WT *Rps. viridis* is too small to be compatible with a direct effect of exchange on the C═O mode of a protonated carboxylic residue. Furthermore, mutations at the Trp L100 or Trp M250 sites that are remote from the side chain of Glu L104 should not influence the frequency of the COOH group of this residue. The ≈1 cm^{-1} downshift upon $^1H/^2H$ exchange of the differential signals that disappears in mutants at the L104 site can be rationalized by invoking a small change in the strength of the Glu L104 hydrogen bond to the 9-keto group of H_A upon deuteration. By slightly altering the positioning of ring V in the protein pocket and/or the electron density on ring V of the H_A molecule, such a change would in turn induce a small downshift of the frequency of the 10a-ester C═O. In an alternative interpretation, the ≈1 cm^{-1} downshift of the 10a-ester C═O could be related to the $^1H/^2H$ exchange of the proton at C_{10}. In this case the exchange itself would depend on the conformation of ring V and thus upon the state of hydrogen bonding of the 9-keto group of H_A. In any case, the present observations further strengthen the notion that the C═O mode of the Glu L104 side chain contributes significantly neither to the Q_A^-/Q_A spectrum nor to the H_A^-/H_A spectrum of WT *Rps. viridis* RCs.[2]

Having identified the dominant contribution of the 10a-ester C═O mode of H_A in the 1750−1700 cm^{-1} region of the Q_A^-/Q_A spectra of *Rps. viridis* RCs via an electrostatic effect, it would seem of interest to search for a similar contribution from the 9-keto C═O vibration, whose mode has been identified at ≈1676 cm^{-1} in the H_A^-/H_A spectrum of WT *Rps. viridis* (Figures 2a and 3a). Such an assignment should be intrinsically on weaker grounds than for the 10a-ester C═O mode as overlapping protein modes are now coming into play in this frequency range. Nevertheless, the WT minus mutant double-difference Q_A^-/Q_A spectra (Figure 6a,b) show a negative band at 1676 cm^{-1}, which probably contains at least some contribution from the 9-keto C═O mode of H_A. In view of the strong band congestion in this spectral range, it is only possible to guess that the negative band at 1676 cm^{-1} should be associated with the positive band at 1685 cm^{-1} rather than with that at 1691 cm^{-1}. In this frame, the effect of Q_A reduction would be to slightly upshift the frequency of the 9-keto C═O of H_A, giving rise to a differential signal at 1676/1685 cm^{-1} in WT RCs and at 1691/1697 cm^{-1} in the EQ(L104) mutant (Figure 6a). Finally, the notion that the frequency of the carbonyls attached to ring V of H_A is sensitive to the electrostatic perturbation induced by the charge on the quinone Q_A has received further support when the effect of the EQ(L104) mutation on the Q_B^-/Q_B spectra of *Rps. viridis* RCs was analyzed (*36*). It was indeed found that the WT minus EQ(L104) signature around 1730 cm^{-1} observed upon Q_B reduction has the same shape as that described upon Q_A reduction but an amplitude reduced by a factor of about 3.

Heterogeneity of the Conformation of Ring V of H_A. In a previous section, the negative bands at 1747 and 1732 cm^{-1} in the H_A^-/H_A spectra of WT *Rps. viridis* (Figure 2a) have been assigned to the 10a-ester C═O mode of two distinct populations of H_A that differ by their conformation at ring V. In view of previous results on *Rb. sphaeroides* RCs bearing the mutation WF(L100), it can be proposed that the band at 1747 cm^{-1} corresponds to a population in which the hydrogen bond between Trp L100 and the 10a-ester C═O of H_A is not established, while for the band at 1732 cm^{-1} this hydrogen bond would be present. The effect of the EQ(L104) mutation and of $^1H/^2H$ exchange on the IR signals corresponding to the main population of H_A in WT *Rps. viridis* with a 10a-ester C═O absorbing at 1732 cm^{-1} shows that for this population the hydrogen bond between Glu L104 and the 9-keto C═O is established. In contrast, the band at 1747 cm^{-1} in the H_A^-/H_A and Q_A^-/Q_A spectra of WT *Rps. viridis* is unaffected by the EQ(L104) mutation, and $^1H/^2H$ exchange leaves the 1747 cm^{-1} signal in the Q_A^-/Q_A spectrum unperturbed. These observations suggest that for this specific population of H_A responsible for the band at 1747 cm^{-1} in the spectra of WT *Rps. viridis* RCs, the hydrogen bond between Glu L104 and the 9-keto C═O may not be established. It should be noticed, however, that in the WF(L100) mutant of *Rb. sphaeroides* the effect of EL(L104) mutation and of $^1H/^2H$ exchange indicates that the 9-keto group of H_A remains hydrogen-bonded to Glu L104 (*35*).

A shoulder is observed at 1725 cm^{-1} in the H_A^-/H_A spectra of WT *Rps. viridis* (Figure 2a). This shoulder is located at the same frequency as the band corresponding to the main population of the 10a-ester C═O of H_A in the EQ(L104) mutant. Similarly, a small differential signal centered at 1725 cm^{-1} in the Q_A^-/Q_A spectrum of WT *Rps. viridis* (Figure 4a) is located under the main differential signal of the EQ(L104) mutant spectrum. It is thus tempting to speculate that these features of the WT spectra correspond to a minor population of H_A molecules having a conformation of their 10a-ester C═O similar to that found in the EQ(L104) mutant. As the frequency of the 1725 cm^{-1} band for the latter population is far from that of a free 10a-ester C═O, it can be further proposed that a hydrogen bonding interaction with Trp L100 exists for this population. Due to the small magnitude of the signals corresponding to this population, their sensitivity to $^1H/^2H$ exchange cannot be reliably estimated. In the case of the WT *Rb. sphaeroides* RCs, a

[2] A small effect of $^1H/^2H$ exchange has been previously described in the 1745−1735 cm^{-1} range of the H_A^-/H_A spectra of WT *Rb. sphaeroides* and *Rps. viridis* RCs (*18*). In addition, a downshift by ≈1 cm^{-1} of the 1732 cm^{-1} band in the H_A^-/H_A spectrum has been observed upon $^1H/^2H$ exchange in the present study (not shown). These effects are at least partly due to the indirect perturbation of the 10a-ester C═O mode of H_A upon exchange of the proton of Glu L104 hydrogen-bonded to the 9-keto group described above. However, a weak direct contribution of the COOH mode of Glu L104 to the 1760−1700 cm^{-1} range of the H_A^-/H_A spectra cannot be totally excluded.

small differential signal centered at ≈1719 cm^{-1} in the Q_A^-/Q_A spectrum and sensitive both to the EL(L104) and WF(L100) mutations and to $^1H/^2H$ exchange has been interpreted in terms of a third population of 10a-ester C═O of H_A (*35*). Thus, on the basis of the effects of $^1H/^2H$ exchange and of the EQ(L104) mutation, the H_A^-/H_A and Q_A^-/Q_A spectra of WT *Rps. viridis* in the region above 1700 cm^{-1} can be interpreted in terms of contributions from the 10a-ester C═O of H_A in three populations of H_A molecules that differ by the hydrogen bonds to the carbonyls of ring V. In a first population with no hydrogen bond the 10a-ester C═O absorbs at 1747 cm^{-1}. In a second population, having hydrogen bonds to both Trp L100 and Glu L104 residues, it absorbs at 1732 cm^{-1}. Finally, in a third population with a hydrogen bond at least to Trp L100, it absorbs at 1725 cm^{-1}. A WF(L100) mutant in *Rps. viridis* would be useful to assess this tentative interpretation.

The WF(M250) mutation affects to different extents the bands assigned to the various contributions of the 10a-ester C═O vibration of H_A in the H_A^-/H_A and Q_A^-/Q_A spectra of WT *Rps. viridis*. The WT minus WF(M250) double-difference spectra (Figures 3b and 6c,d) indicate that the largest effect is on the population corresponding to the 1732 cm^{-1} band of WT that upshifts by ≈2 cm^{-1} in the mutant. The effect on the 1747 cm^{-1} bands of WT is just barely detectable above the noise in the Q_A^-/Q_A double-difference spectra (Figure 6c,d), although it appears more clearly in the H_A^-/H_A double-difference spectra (Figure 3b). There seems to be an influence (Figure 6c) on the population responsible for the small differential signal at 1727/1723 cm^{-1} in the Q_A^-/Q_A spectrum of WT *Rps. viridis*. The changes observed around 1640 cm^{-1} in the Q_A^-/Q_A spectrum of the WF(M250) mutant (Figure 6c,d) and the isotope effects on the quinone vibrations associated with these changes (unpublished results) indicate that a small displacement of the Q_A molecule has taken place in the mutant. It is always possible that the overall structure of the Q_A and H_A binding sites have been slightly altered, leading to the perturbation of the 10a-ester C═O vibration of H_A. However, there are two observations that point to only limited structural changes upon the WF(M250) mutation. On one hand, the effect of $^1H/^2H$ exchange indicates that the hydrogen bond to the 9-keto group of H_A is maintained (Figure 7c). On the other hand, the response of the protein to Q_A reduction, which is responsible for most of the large signals between 1680 and 1650 cm^{-1} in the Q_A^-/Q_A spectra, appears little affected by the mutation. It is thus more probable that the van der Waals contact between Trp M250 and the 10a-ester C═O group of H_A in WT RCs is one of the factors taking part in the various conformations of this ester group. The WF(M250) mutation would then slightly perturb the geometry of these conformations.

As noticed in the Results section, the H_A^-/H_A and Q_A^-/Q_A spectra show a large number of bands that appear at the same position, although with different amplitudes, for both WT and the EQ(L104) mutant. One such case has been discussed above regarding the small population of H_A in WT RCs with the 10a-ester C═O absorbing at 1725 cm^{-1} and having the same conformation as the main population in the mutant. Similarly, the small population of 10a-ester C═O of H_A absorbing at 1732 cm^{-1} in EQ(L104) corresponds to the main population observed in WT RCs and could be related to a fraction of H_A with the 9-keto group forming a hydrogen bond with Gln L104. Taking into account the results from the present FTIR study on the effect of changing the Glu L104 and Trp M250 residues interacting with the ring V of H_A of *Rps. viridis* and from an analogous study on altering the Glu L104 and Trp L100 residues of *Rb. sphaeroides* (*35*), one may propose a framework to help rationalize such heterogeneity. In this model, the hydrogen bonds between, on one hand, the 9-keto C═O of H_A and Glu L104 and, on the other hand, Trp L100 and the 10a-ester C═O (Figure 1) may not always both be established simultaneously. Indeed, if the hydrogen bond between the 9-keto C═O of a subpopulation of H_A and Glu L104 in WT RCs is broken (whether on a static or dynamic basis), it is normal to expect in the H_A^-/H_A and Q_A^-/Q_A spectra of WT contributions from a free 9-keto C═O of H_A at 1693−1695 cm^{-1}, i.e., at the same frequency as found in the EQ(L104) mutant. The same situation seems to apply also for the H_A^- anion mode in the H_A^-/H_A spectra, where the fraction of H_A^- free from interaction with Glu L104 can be expected to absorb at 1627 cm^{-1} (Figure 3a), just like in the EQ(L104) mutant. Furthermore, the splitting of the 9-keto C═O anion mode at 1602 and 1595 cm^{-1} in WT RCs (Figures 2a and 3a) is indicative of more than one conformation of H_A. In addition, other residues such as Trp M250, which is in van der Waals contact with ring V, can further modulate the conformation of the substituents. It is, however, unclear whether the localized conformational changes occurring upon mutations that disrupt hydrogen-bonding interactions to the carbonyls on ring V of H_A are primarily due to the modification of the electron density in the macrocycle or to a repositioning of the cofactor in the protein pocket.

Comparison with Other Spectroscopic Results and Implications for Electron Transfer. A structural heterogeneity related to the conformation of the 10a-ester C═O on ring V of H_A has been initially reported on the basis of the effect of the EL(L104) and WF(L100) mutations on the Q_A^-/Q_A FTIR difference spectra of WT *Rb. sphaeroides* RCs (*35*). By use of resonance Raman spectroscopy, conformational heterogeneity of the 10a-ester C═O and the 2a-acetyl groups of at least one of the two BPh molecules has been described in the RC of *Rb. capsulatus* (*48*). Importantly, it was shown that disruption of the hydrogen bond between the 9-keto C═O of H_A and Glu L104 alters the geometry both of the 10a-ester C═O group of H_A (*35*, *48*) and of the 2a-acetyl group on ring I at the opposite side of the H_A macrocycle from the 9-keto C═O (*48*).

The existence of at least two distinct conformations of the H_A^- state in the RCs of *Rps. viridis* RCs has been initially proposed by Tiede et al. (*49*) in order to explain a large irreversible change of the optical spectra that accompanies the rewarming of *Rps. viridis* RCs trapped in the H_A^- state at low temperature. On the basis of ENDOR experiments on freeze-trapped H_A^- states obtained in various mutants of *Rb. sphaeroides*, Müh et al. (*46*) have recently attributed this conformational change to a reorientation of the 2a-acetyl group of H_A upon rewarming. In WT RCs, two conformations of H_A^- that differ by the orientation of the 2a-acetyl group would be already present. By investigating the ENDOR spectra of RCs bearing mutations affecting the native environment of the 9-keto, 10a-ester, and 2a-acetyl groups of H_A, it was further concluded that the relative

contribution of the two conformers of H_A^- and/or their precise geometry are under the influence of the presence or absence of hydrogen bonds to those three carbonyl groups of H_A (*46*, *50*). Furthermore, the nature of the residue at M210 (equivalent to M208 in *Rps. viridis*), which is located close to the 2a-acetyl group of H_A (Figure 1) and occupies a critical position between P, B_A, and H_A, appears to have a direct influence on the conformation of this acetyl (*50*). While mutation of Tyr M210 to Phe or Trp has no effect on the two conformations of H_A^- found in native RCs, its replacement by a Leu side chain, which probably exerts steric hindrance on the 2a-acetyl group of H_A, would lead to only one of the two conformations. Similarly, the replacement of Tyr M210 by a His side chain, which could form a hydrogen bond to the 2a-acetyl, would lead to only one conformation that differs from those found in native RCs (*50*). FTIR studies of the YF(M208) and YL(M208) mutants of *Rps. viridis* are being considered in order to investigate the effect of the nature of the residue at M208 on the conformation of the 10a-ester C═O group of H_A. Such studies might also provide information leading to an assignment for the IR band of the 2a-acetyl group of H_A, which is still missing due to spectral congestion.

The present results indicating the existence of three discrete conformations of the 10a-ester C═O of H_A in WT *Rps. viridis* corresponding to different states of hydrogen-bonding interaction of the 9-keto and 10a-ester C═O groups with the RC protein extend our previous observation of a similar heterogeneity of H_A in *Rb. sphaeroides* (*35*). Taken together with the newly reported evidence of heterogeneity of the conformation of the 2a-acetyl group obtained by resonance Raman on H_A (*48*) and by ENDOR on H_A^- (*46*, *50*), a new picture of H_A emerges, characterized by a multiplicity of discrete conformational states in both the neutral and reduced forms. Such heterogeneity of the electronic structure of H_A has direct implications for electron transfer. The influence of the conformation of the 2a-acetyl group of H_A on the charge repartition within the macrocycle has long been recognized (*51*). Similarly, the hydrogen bonds to the carbonyls of ring V of H_A, by affecting the conformation of ring V, should modulate the redox potential of the molecule (*51*). Thus, the multiplicity of electronic structures can be expected to lead to different rates for the electron transfer in and out of H_A as it has been observed experimentally (*52*−*55*). In addition, it is possible that the various conformations that are described here for the static states H_A and H_A^- participate actively in the stabilization of charges during the electron-transfer process itself. Small molecular changes such as strengthening or weakening of the hydrogen bonds between Glu L104 and the 9-keto C═O and between Trp L100 and the 10a-ester C═O, an alteration of the interaction between Trp M250 and the 10a-ester C═O, or a rotation of the 2a-acetyl or 10a-carbomethoxy groups could play a determinant role during the formation of H_A^- and the subsequent relaxation processes. As discussed previously by Müh et al. (*46*, *50*) for the rotation of the 2a-acetyl group of H_A, all these conformational changes could constitute "molecular switches" activated by the presence of the positive charge on P^+.

The structural heterogeneity of H_A is to be related to the well-established distribution of the free energy of the state $P^+H_A^-$ (*54*, *56*) as well as to the notion of "dynamic solvation" or "conformational cooling" of the $P^+H_A^-$ radical pair giving rise to the nonexponentiality of the spontaneous or stimulated emission from P* (*57*−*61*). The nonexponentiality of the kinetics involving H_A^- can be also at least partly related to the heterogeneity in the reorganization energy associated with the electron transfer. Our data demonstrate that the frequency of several modes of H_A is altered upon Q_A reduction. The multiplicity of the conformation of the substituents of H_A will contribute a large number of internal relaxation modes to the reorganization energy accompanying electron transfer.

Absence of Protonation Changes of Carboxylic Residues upon Q_A Reduction. In the spectral range 1770−1700 cm^{-1}, where protonated carboxylic amino acid residues normally absorb, the Q_A^-/Q_A spectrum of the EQ(L104) mutant shows no effect of $^1H/^2H$ exchange (Figure 7b). This observation provides compelling evidence that in this mutant no exchangeable protonated carboxylic residue undergoes protonation change upon Q_A reduction. As discussed in a previous section, the differential signal centered at ≈1730 cm^{-1} in the ^1H_2O minus ^2H_2O Q_A^-/Q_A double-difference spectrum of WT *Rps. viridis* (Figure 7a) that is absent in the corresponding spectrum of the EQ(L104) mutant (Figure 7b) cannot be due to the direct contribution from a carboxylic residue. It is rather assigned to an indirect effect combining (i) $^1H/^2H$ exchange either at the C_{10} proton or at the hydrogen bond between Glu L104 and the ring V of H_A that slightly shifts the frequency of the 10a-ester C═O of H_A and (ii) an electrostatic effect of Q_A reduction on the frequency of the 10a-ester C═O of H_A. On the basis of estimates of the extinction coefficients of carboxylic acids and of semiquinones (*26*, *35*) compared to the noise level of the FTIR measurements (Figure 7b), it can be estimated that a lower limit of ≈0.02 H^+/Q_A^- would be detected. This limiting value of proton uptake by carboxylic residues has to be compared to the values of proton uptake by Glu residues that have been predicted on the basis of electrostatic calculations at 0.35 H^+/Q_A^- (*33*) or 0.07 H^+/Q_A^- (*34*). Note that a discrepancy between the predictions from electrostatic calculations (*31*) and the FTIR results has also been noticed for Q_A photoreduction in *Rb. sphaeroides* (*35*). Similarly, for Q_B photoreduction in *Rps. viridis*, the electrostatic calculations predict proton *uptake* by carboxylic of 0.5−0.6 H^+/Q_B^- (*33*, *34*), while a small proton *release* of ≈0.1 H^+/Q_B^- by a carboxylic group has been reported (*62*). Only in the case of Q_B photoreduction in *Rb. sphaeroides* has proton uptake by a carboxylic group been observed by FTIR and assigned to Glu L212 on the basis of studies with mutants (*26*, *27*). While the latter experimental result had been considered to support, at least partially, the electrostatic calculations (*30*, *31*), a more recent set of calculations in *Rb. sphaeroides* (*32*) is no longer in agreement with the FTIR results. A possible explanation for this general lack of agreement based on the observation of the IR signatures for highly polarizable hydrogen-bond networks in the Q_A^-/Q_A and Q_B^-/Q_B spectra and suggesting that the protons taken up upon quinone reduction tend to reside more on the bound water molecules of the network than on the carboxylic groups themselves has been presented (*41*).

In conclusion, the effect of the EQ(L104) and WF(M250) or WY(M250) mutations on the H_A^-/H_A FTIR spectra is consistent with the nature of the interactions between the

corresponding residues and the H_A molecule proposed in the X-ray models of the RC. The spectral changes induced by the mutations allow specific IR bands to be assigned to the 9-keto and 10a-ester C═O modes of H_A and H_A^-. The Q_A^-/Q_A spectra measured on the WT and mutant RCs demonstrate a pronounced electrostatic influence of Q_A reduction on the 10a-ester C═O IR mode of H_A. On the other hand, there is no direct contribution of the C═O mode of any exchangeable protonated carboxylic residue to the Q_A^-/Q_A spectra. The combined H_A^-/H_A and Q_A^-/Q_A results show that the 10a-ester C═O mode of H_A occupies several discrete conformations that appear to depend on the precise interactions of the cofactor with the protein and, notably, the presence or absence of the hydrogen bond between Glu L104 and the 9-keto C═O of H_A, the van der Waals contact with Trp M250, and most probably the presence of the hydrogen bond between Trp L100 and the 10a-ester C═O of H_A. These different conformations of the 10a-ester C═O of H_A might be related to the well-documented heterogeneity of the kinetics of electron transfer in and out of H_A. If this were the case, our results would provide a direct link between structural and functional heterogeneity in bacterial RCs.

ACKNOWLEDGMENT

We acknowledge discussions with Frank Müh and Wolfgang Lubitz and thank Frank Whitby for his help with the computer graphic program to draw Figure 1.

REFERENCES

1. Michel, H., Epp, O., and Deisenhofer, J. (1986) *EMBO J. 5*, 2445−2451.
2. Deisenhofer, J., and Michel, H. (1989) *EMBO J. 8*, 2149−2169.
3. Lancaster, C. R. D., Ermler, U., and Michel, H. (1995) in *Anoxygenic Photosynthetic Bacteria* (Blankenship, R. E., Madigan, M. T., and Bauer, C. E., Eds.) pp 503−526, Kluwer Academic Publishers, Dordrecht, The Netherlands.
4. Lancaster, C. R. D., and Michel, H. (1997) *Structure 5*, 1339−1359.
5. Allen, J. P., Feher, G., Yeates, T. O., Komiya, H., and Rees, D. C. (1988) *Proc. Natl. Acad. Sci. U.S.A. 85*, 8487−8491.
6. Yeates, T. O., Komiya, H., Chirino, A., Rees, D. C., Allen, J. P., and Feher, G. (1988) *Proc. Natl. Acad. Sci. U.S.A. 85*, 7993−7997.
7. Feher, G., Allen, J. P., Okamura, M. Y., and Rees, D. C. (1989) *Nature 339*, 111−116.
8. El-Kabbani, O., Chang, C.-H., Tiede, D., Norris, J., and Schiffer, M. (1991) *Biochemistry 30*, 5361−5369.
9. Ermler, U., Fritzsch, G., Buchanan, S., and Michel, H. (1994) *Structure 2*, 925−936.
10. Arnoux, B., and Reiss-Husson, F. (1996) *Eur. Biophys. J. 24*, 233−242.
11. Plato, M., Michel-Beyerle, M.-E., Bixon, M., and Jortner, J. (1989) *FEBS Lett. 249*, 70−74.
12. Parson, W. W., Chu, Z. T., and Warshel, A. (1990) *Biochim. Biophys. Acta 1017*, 251−272.
13. Gray, K. A., Farchaus, J. W., Wachtveitl, J., Breton, J., Finkele, U., Lauterwasser, C., Zinth, W., and Oesterhelt, D. (1990) in *Reaction Centers of Photosynthetic Bacteria* (Michel-Beyerle, M.-E., Ed.) pp 251−264, Springer-Verlag, Berlin.
14. Stilz, H. U., Finkele, U., Holzapfel, W., Lauterwasser, C., Zinth, W., and Oesterhelt, D. (1990) in *Reaction Centers of Photosynthetic Bacteria* (Michel-Beyerle, M.-E., Ed.) pp 265−271, Springer-Verlag, Berlin.
15. Coleman, W. J., Bylina, E. J., Aumeier, W., Siegl, J., Eberl, U., Heckmann, R., Ogrodnik, A., Michel-Beyerle, M.-E., and Youvan, D. C. (1990) in *Reaction Centers of Photosynthetic Bacteria* (Michel-Beyerle, M.-E., Ed.) pp 273−282, Springer-Verlag, Berlin.
16. Nabedryk, E., Mäntele, W., Tavitian B., and Breton, J. (1986) *Photochem. Photobiol. 43*, 461−465.
17. Nabedryk, E., Andrianambinintsoa, S., Mäntele, W., and Breton, J. (1988) in *The Photosynthetic Bacterial Reaction Center: Structure and Dynamics* (Breton, J., and Verméglio, A., Eds.) pp 237−250, Plenum Press, New York.
18. Nabedryk, E., Andrianambinintsoa, S., Dejonghe, D., and Breton, J. (1995) *Chem. Phys. 194*, 371−378.
19. Mäntele, W., Wollenweber, A., Nabedryk, E., and Breton, J., (1988) *Proc. Natl. Acad. Sci. U.S.A. 85*, 8468−8472.
20. Breton, J., Thibodeau, D. L., Berthomieu, C., Mäntele, W., Verméglio, A., and Nabedryk, E. (1991) *FEBS Lett. 278*, 257−260.
21. Breton, J., Burie, J.-R., Berthomieu, C., Thibodeau, D. L., Andrianambinintsoa, S., Dejonghe, D., Berger, G., and Nabedryk, E. (1992) in *The Photosynthetic Bacterial Reaction Center II: Structure, Spectroscopy, and Dynamics* (Breton, J., and Verméglio, A., Eds.) pp 155−162, Plenum Press, New York.
22. Breton, J., Burie, J.-R., Berthomieu, C., Berger, G., and Nabedryk, E. (1994) *Biochemistry 33*, 4953−4965.
23. Breton, J., Bauscher, M., Berthomieu, C., Thibodeau, D. L., Andrianambinintsoa, S., Dejonghe, D., Mäntele, W., and Nabedryk, E. (1991) in *Spectroscopy of Biological Molecules* (Hester, R. E., and Girling, R. B., Eds.) pp 43−46, The Royal Society of Chemistry, Cambridge, England.
24. Breton, J. (1997) *Proc. Natl. Acad. Sci. U.S.A. 94*, 11318−11323.
25. Nabedryk, E. (1996) in *Infrared Spectroscopy of Biomolecules* (Mantsch, H. H., and Chapman, D., Eds.) pp 39−81, Wiley-Liss, New York.
26. Nabedryk, E., Breton, J., Hienerwadel, R., Fogel, C., Mäntele, W., Paddock, M. L., and Okamura, M. Y. (1995) *Biochemistry 34*, 14722−14732.
27. Nabedryk, E., Breton, J., Okamura, M. Y., and Paddock, M. L. (1998) *Biochemistry 37*, 14457−14462.
28. Rothschild, K. (1992) *J. Bioenerg. Biomembr. 24*, 147−167.
29. Siebert, F. (1993) in *Methods in Enzymology, Biochemical Spectroscopy* (Sauer, K., Ed.) Vol. 246, pp 501−526, Academic Press, San Diego, CA.
30. Gunner, M. R., and Honig, B. (1992) in *The Photosynthetic Bacterial Reaction Center II: Structure, Spectroscopy, and Dynamics* (Breton, J., and Verméglio, A., Eds.) pp 403−410, Plenum Press, New York.
31. Beroza, P., Fredkin, D. R., Okamura, M. Y., and Feher, G. (1995) *Biophys. J. 68*, 2233−2250.
32. Alexov, E. G., and Gunner, M. R. (1999) *Biochemistry 38*, 8253−8270.
33. Lancaster, C. R. D., Michel, H., Honig, B., and Gunner, M. R. (1996) *Biophys. J. 70*, 2469−2492.
34. Rabenstein, B., Ullman, G. M., and Knapp, E.-W. (1998) *Biochemistry 37*, 2488−2495.
35. Breton, J., Nabedryk, E., Allen, J. P., and Williams, J. C. (1997) *Biochemistry 36*, 4515−4525.
36. Breton, J., Bibikova, M., Oesterhelt, D., and Nabedryk, E. (1998) in *Photosynthesis: Mechanisms and Effects* (Garab, G., Ed.) Vol. II, pp 687−692, Kluwer Academic Publishers, Dordrecht, The Netherlands.
37. Kunkel, T. A. (1985) *Proc. Natl. Acad. Sci. U.S.A. 82*, 488−492.
38. Laussermair, E., and Oesterhelt, D. (1992) *EMBO J. 11*, 777−783.
39. Arlt, T., Dohse, B., Schmidt, S., Wachtveitl, J., Laussermair, E., Zinth, W., and Oesterhelt, D. (1996) *Biochemistry 35*, 9235−9244.
40. Breton, J., and Nabedryk, E. (1995) in *Photosynthesis: from Light to Biosphere* (Mathis, P., Ed.) pp 395−400, Kluwer Academic Publishers, Dordrecht, The Netherlands.

41. Breton, J., and Nabedryk, E. (1998) *Photosynth. Res. 55*, 301−307.
42. Lutz, M., and Mäntele, W. (1991) in *Chlorophylls* (Scheer, H., Ed.) pp 855−902, CRC Press, Boca Raton, FL.
43. Socrates, G. (1994) *Infrared Characteristic Group Frequencies*, 2nd ed., Wiley and Sons, New York.
44. Lubitz, W., Bönigk, B., Plato, M., Isaacson, R. A., Okamura, M. Y., and Feher, G. (1990) in *Current Research in Photosynthesis* (Baltscheffsky, M., Ed.) Vol. I, pp 141−144, Kluwer Academic Publishers, Dordrecht, The Netherlands.
45. Zhou, Q., Robert, B., and Lutz, M. (1989) *Biochim. Biophys. Acta 977*, 10−18.
46. Müh, F., Williams, J. C., Allen, J. P., and Lubitz, W. (1998) *Biochemistry 37*, 13066−13074.
47. Nabedryk, E., Andrianambinintsoa, S., Berger, G., Leonhard, M., Mäntele, W., and Breton, J. (1990) *Biochim. Biophys. Acta 1016*, 49−54.
48. Cua, A., Kirmaier, C., Holten, D., and Bocian, D. (1998) *Biochemistry 37*, 6394−6401.
49. Tiede, D. M., Kellog, E., and Breton, J. (1987) *Biochim. Biophys. Acta 892*, 294−302.
50. Müh, F., Jones, M. R., and Lubitz, W. (1999) *Biospectroscopy 5*, 35−46.
51. Hanson, L. K., Thompson, M. A., Zerner, M. C., and Fajer, J. (1988) in *The Photosynthetic Bacterial Reaction Center: Structure and Dynamics* (Breton, J., and Verméglio, A., Eds.) pp 355−367, Plenum Press, New York.
52. Kirmaier, C., and Holten, D. (1990) *Proc. Natl. Acad. Sci. U.S.A. 87*, 3552−3556.
53. Woodbury, N. W., and Allen, J. P. (1995) in *Anoxygenic Photosynthetic Bacteria* (Blankenship, R. E., Madigan, M. T., and Bauer, C. E., Eds.) pp 527−557, Kluwer Academic Publishers, Dordrecht, The Netherlands.
54. Woodbury, N. W. T., and Parson W. W. (1984) *Biochim. Biophys. Acta 767*, 345−361.
55. Sebban, P., and Wraight, C. A. (1989) *Biochim. Biophys. Acta 974*, 54−65.
56. Ogrodnik, A., Keupp, W., Volk, M., Aumeier, G., and Michel-Beyerle, M. E. (1994) *J. Phys. Chem. 98*, 3432−3439.
57. Small, G., Hayes, J. M., and Silbey, R. J. (1992) *J. Phys. Chem. 96*, 7499−7501.
58. Jia, Y., DiMagno, T. J., Chan, C.-K., Wang, Z., Du, M., Hanson, D. K., Schiffer, M., Norris, J. R., Fleming, G. R., and Popov, M. S. (1993) *J. Phys. Chem. 97*, 13180−13191.
59. Peloquin, J. M., Williams, J. C., Lin, X., Alden, R. G., Taguchi, A. K. W., Allen, J. P., and Woodbury, N. W. (1994) *Biochemistry 33*, 8089−8100.
60. Holzwarth, A. R., and Müller, M. G., (1996) *Biochemistry 35*, 11820−11831.
61. van Stokkum, I. H. M., Beekman, L. M. P., Jones, M. R., van Brederode, M. E., and van Grondelle, R. (1997) *Biochemistry 36*, 11360−11368.
62. Breton, J., Nabedryk, E., Mioskowski, C., and Boullais, C. (1996) in *The Reaction Center of Photosynthetic Bacteria* (Michel-Beyerle, M.-E., Ed.) pp 381−394, Springer, Berlin.

BI990927F